Structural and energetic parallels between hydrogenated and fluorinated fullerenes: $C_{36}X_6$

Thomas Heine,[a] Patrick W. Fowler,[a] Kevin M. Rogers[a] and Gotthard Seifert[b]

[a] *School of Chemistry, University of Exeter, Stocker Road, Exeter, UK EX4 4QD*
[b] *Universität-GH Paderborn, FB6 Theoretische Physik, D-33095 Paderborn, Germany*

Received (in Cambridge) 18th January 1999, Accepted 3rd February 1999

An exhaustive search of $C_{36}H_6$ and symmetrical $C_{36}F_6$ isomers based on the cylindrical C_{36} fullerene predicts the same D_{3h} structure to have the lowest energy in each series. Some competitive structures of $C_{36}H_6$ have only trivial symmetry but share the feature of 1,4 pairing of addends with the best isomer. Isostructural $C_{36}X_6$ (X = H, F) molecules are predicted to have constant energy difference. All 84 000 geometry optimisations reported here used the DFTB model, with checking of the new parameters for C/F and F/F interactions against LDA and GGA full density-functional methods.

1 Introduction

A number of hydrogenated and halogenated fullerene cages have been characterised in recent years[1–4] and parallels in the extent and pattern of addition have been noted for both C_{60} and C_{70} derivatives. For example, $C_{60}H_{18}$ and $C_{60}F_{18}$ are thought to have the same C_{3v} structure.[5] Some theoretical work on the energies of cages has lent support to this idea, but has explored only a limited number of cases.[6] In order to decide if the observed parallels are part of a more general trend, it is clearly desirable to consider a much larger test set.

Extensive comparisons of optimised structures and energies for molecules as large as this are potentially expensive but fortunately an economical and semi-quantitatively accurate method for their computation is already available. The DFTB (density-functional tight-binding) method combines the economy of tight-binding with an accuracy approaching that of full density-functional theory. It requires parameterisation for each chemical combination of elements, but this can be done in a straightforward way. The DFTB method has been used successfully, without further adjustment, for fullerenes and other carbon cages,[7–10] heteronuclear BN cages[11,12] and hydrocarbons.[13] Here we report the determination of the parameters necessary to extend the method to fluorocarbons and we use DFTB to identify low-energy forms of $C_{36}H_6$ and $C_{36}F_6$ so that comparisons in energy and structure can be made across the whole range of isomers.

Our test case for comparison of isostructural C_nH_m and C_nF_m isomers is the C_{36} cage and its addition compounds $C_{36}X_6$. C_{36} has become a topical small fullerene, with the claim that it may be possible to prepare it in the form of a tightly bound solid;[14] the building block for proposed $(C_{36})_\infty$ solids[15] is the cylindrical D_{6h} fullerene which may also exhibit its characteristic hexavalence by picking up six hydrogen atoms. An extensive computational study of hypothetical $C_{36}H_6$ isomers identified a low-energy D_{3h} candidate for this molecule.[15] In that work, some 1885 isomeric $C_{36}H_6$ isomers were optimised with DFTB and this set is here extended for complete coverage of all 82 123 possibilities. In the present paper, we discuss the survey of $C_{36}H_6$ isomers and explore the H/F parallels, taking as the basis for comparison the set of all 1885 $C_{36}H_6$ and $C_{36}F_6$ cages that are based on the cylindrical fullerene and have any symmetry higher than the trivial C_1.

The structure of the paper is as follows. Section 2 describes the determination of C/F and F/F parameters for the DFTB model. These are tested against full density-functional calculations and experimental results for small fluorocarbons in Section 3. Section 4 describes the generation of all possible $C_{36}X_6$ addition patterns for cylindrical C_{36}. In Section 5, the results of the DFTB calculations are described, first for the full set of $C_{36}H_6$ isomers and then for the H/F comparison set. Finally, they are compared with full DFT calculations on a small number of cage isomers.

2 Determination of parameters

The DFTB method is based on a linear combination of atomic orbitals (LCAO) Ansatz for the Kohn–Sham molecular orbitals ψ_i as a combination of basis functions φ_ν centred at the atomic sites[16,17] [eqn. (1)]. Several atomic orbitals φ_ν may correspond to

$$\psi_i = \sum c_\nu^i \varphi_\nu \tag{1}$$

any one site. For C and F sites these are 2s and 2p functions, each represented as a contraction of Slater-type orbitals. The expansion coefficients c_ν^i in eqn. (1) are found by solving the Kohn–Sham secular problem given in eqn. (2), which is

$$\sum_\mu c_\mu^i (F_{\mu\nu} - \varepsilon_i S_{\mu\nu}) = 0 \quad \forall \nu \tag{2}$$

expressed in terms of the Kohn–Sham matrix elements $F_{\mu\nu} = \langle\varphi_\mu|\hat{T} + V_{\text{eff}}|\varphi_\nu\rangle$ and overlap matrix elements $S_{\mu\nu} = \langle\varphi_\mu|\varphi_\nu\rangle$. The effective potential V_{eff} is a sum of atomic contributions, each determined by an LDA–DFT calculation on a fictitious spherical pseudo-atom, subjected to an additional potential $(r/r_0)^n$. This extra potential was introduced by Eschrig[18] to improve LCAO–LDA band-structure calculations on metals and has a beneficial effect on quantitative binding energies[13] through its compression of the basis functions and electron densities of the pseudo-atoms. The valence wave functions and the effective potential are both taken from the pseudo-atomic calculation. With this approximation,[19] it is necessary to consider only two-centre elements of the Kohn–Sham matrix in eqn. (3),

$$F_{\mu\nu} = \begin{cases} \langle\varphi_\mu|\hat{T} + V_j + V_k|\varphi_\nu\rangle & \text{for } j \neq k \\ \varepsilon_\mu & \text{for } \mu = \nu \\ 0 & \text{otherwise} \end{cases} \tag{3}$$

containing the effective potentials V_j, V_k of the atoms j and k that carry functions φ_μ and φ_ν. In the case of $j = k$, the one-particle energies of the free atom ε_μ are used, giving the correct reference energy in the dissociation limit. Restriction to two-centre terms leads to a Kohn–Sham matrix similar to empirically parameterised non-orthogonal tight-binding schemes, but

Table 1 Bond lengths R (Å), bond angles (°) and atomisation energies E^a (kJ mol^{-1}) of small molecules C_xF_y. Experimental values of geometric parameters are taken from ref. 28. The LDA–LSDA correction for carbon is 1.21 eV (calculated with *AllChem*, VWN, DZVP) and 1.12 eV (calculated with Servedio's program[26] using a Perdew-Zunger potential.[27] For fluorine, the correction can be calculated (for technical reasons) only with the latter code, and is 0.38 eV. For carbon, the *AllChem* value is used

		Geometric parameters				Atomisation energies		
Molecule		DFTB	LDA	GGA	Experiment	E^a_{DFTB}	E^a_{LDA}	E^a_{GGA}
F_2	R_{FF}	1.393	1.393	1.461	1.412	385.9	323.6	223.4
CF_4	R_{CF}	1.328	1.326	1.356	1.323	2871.6	2476.6	2133.9
C_2F_2	R_{CC}	1.205	1.203	1.200		2154.2	1996.8	1889.5
	R_{CF}	1.246	1.285	1.304				
C_2F_4	R_{CC}	1.319	1.333	1.340	1.310	3358.9	3083.7	2765.3
	R_{CF}	1.319	1.317	1.345	1.319			
	$\angle_{FCF}$	112.0	113.8	113.3	112.4			
C_2F_6	R_{CC}	1.520	1.545	1.591	1.545	4606.2	4498.5	3568.5
	R_{CF}	1.347	1.332	1.363	1.326			
	$\angle_{CCF}$	111.9	111.5	109.9	109.8			
C_6F_6	R_{CC}	1.392	1.393	1.405		7359.0	7171.2	6592.2
	R_{CF}	1.321	1.326	1.365				

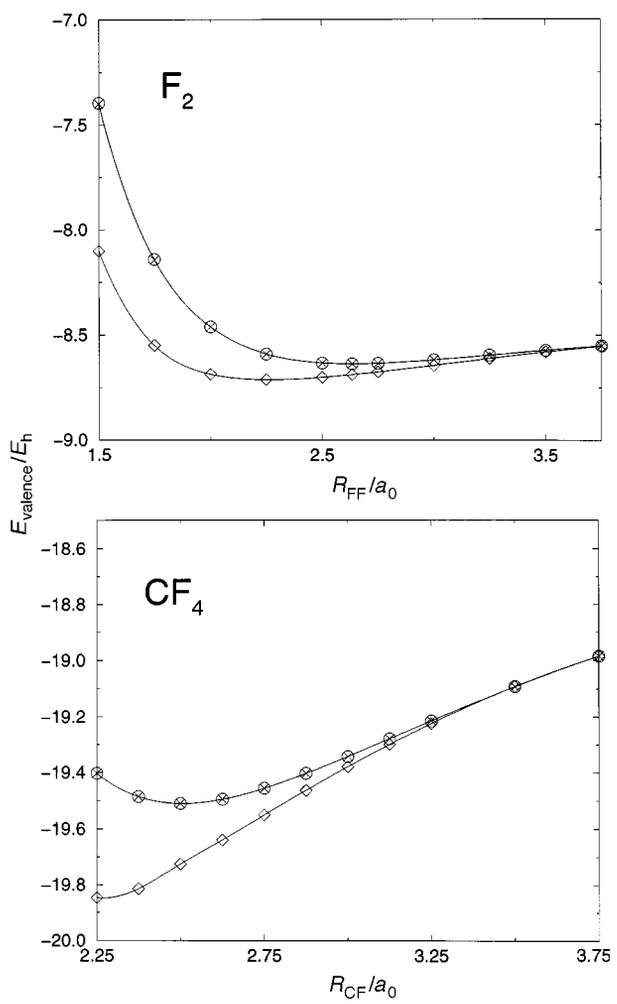

Fig. 1 Parameterisation of F/F and C/F potentials in DFTB. The curves for the two test molecules show the bond length dependence of LDA energies (×), sums of one-particle Kohn–Sham energies (◇) and full DFTB energies including the fitted repulsive potentials (○).

all parameters are obtained here from LDA–DFT calculations. After solving the secular equations for the single particle energies ε_i and eigenstates of the system, the total energy is written as a sum of energies of occupied Kohn–Sham states and a repulsive, short-range, two-particle interaction U[13,20] [eqn. (4)].

$$E = \sum_i^{occ} \varepsilon_i + \tfrac{1}{2} \sum_{j \neq k} U_{jk}(R_{jk}) \qquad (4)$$

Following ref. 13, the repulsive energies for the different atom-type combinations are derived as universal, short-range potentials by fitting the curves of the differences between the sum of energies of occupied Kohn–Sham states and LDA cohesive energy for a reference molecule.

We applied this scheme for carbon and fluorine. The radius r_0 for fluorine was chosen in the same way as for carbon[13] [r_0(C) = 2.7 a_0, r_0(F) = 2.5 a_0], and is about twice the covalent radius of the atom. The reference molecules used for fitting the repulsive potential were F_2 and CF_4. For the carbon–carbon and carbon–hydrogen interactions, the data given in ref. 13 were used.

Fig. 1 presents curves for the bond-length dependence of LDA reference energies, sums of one-particle Kohn–Sham energies and DFTB energies in the new parameterisation.

3 Benchmark calculations

Table 1 reports the results of a comparison between DFTB, two self-consistent DFT methods (LDA and its gradient-corrected form GGA) and experiment for six test molecules. The full DFT calculations were performed with the program package *AllChem*.[21] In what follows, LDA designates calculations performed using a Vosko–Wilk–Nusair exchange-correlation functional,[22] a DZVP basis set[23] and an A2 auxiliary basis set, whereas GGA calculations are those performed with the Becke88-LYP functional,[24,25] a TZVP basis set[23] and *AllChem*'s GEN-A3 automatic generator for auxiliary basis functions (except for $C_{36}F_6$ where the A2 auxiliary basis set was used).

The reference molecules (F_2, CF_4, C_2F_2, C_2F_4, C_2F_6 and C_6F_6) are chosen to sample C–F interactions for carbon in all three hybridisations. In Table 1, the geometries are compared with DFTB calculations in the present C/F and F/F parameterisation. The atomisation energies in the same table are obtained with LSDA-corrected total energies of free spherical atoms.[26,27] The overall picture from Table 1 is encouraging as it shows that the new DFTB parameters give bond lengths and angles in excellent agreement both with experiment[28] and with more sophisticated DFT calculations.

DFTB atomisation energies are generally close to the values from LDA calculations (with errors of < 10% for all but CF_4 and F_2). Both DFTB and LDA values of these quantities could be improved, as shown by the comparison with the more sophisticated GGA model.

4 Generation of the isomers

The DFTB model including the new parameters was used in a complete survey of all possible addition patterns $C_{36}X_6$ formed

by decoration of the D_{6h} fullerene (36:15[29]), the cage implicated in the explanation of the experiments on C_{36} solids.[14]

$C_{36}X_6$ isomers were found by labelling the atoms of the cage and then generating all 36!/(30!6!) binary sequences made up of thirty 0 digits and six 1 digits, the positions of the latter corresponding to the locations of the addends on the cage. Each of the 1 947 792 codes was reduced to its lexicographically smallest value and the symmetry of the corresponding isomer found by applying the 24 projection operators of the D_{6h} point group. All repeated codes were filtered out of the original list and the resulting unique isomers sorted into point group sets. The 82 123 $C_{36}X_6$ isomers produced in this way are classified by maximal point group as 3 D_{3h}, 3 D_{3d}, 3 C_{6v}, 4 C_{3v}, 21 C_{2h}, 46 C_{2v}, 4 C_3, 57 C_i, 439 C_2, 1305 C_s and 80 238 C_1.

The subset of $C_{36}H_6$ with non-trivial symmetry was treated in our previous paper,[15] and here the calculations were extended to include the C_1 isomers that in fact form the majority of the possibilities. Calculations on $C_{36}F_6$ were restricted to the smaller set of 1885 symmetrical isomers.

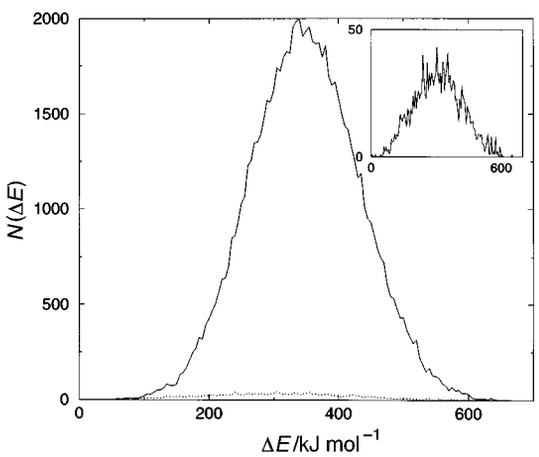

Fig. 2 Distribution of relative energies of isomers $C_{36}H_6$ based on the cylindrical fullerene cage. The full curve shows the distribution for all symmetries based on a 5 kJ mol^{-1} bin size. The dotted and inset curves show the distribution for the 2.3% of isomers with non-trivial symmetry.

Starting coordinates for each isomer were generated as follows. Coordinates for the carbon atoms were obtained by DFTB optimisation of the bare C_{36} fullerene itself, with the origin located at the centre of the cage. Coordinates of the addends were found by extending the radial vectors of the carbon atoms. Initial C–X bond lengths were set at 1.10 Å for hydrogen and 1.33 Å for fluorine. Full DFTB optimisation was then performed. The conjugate-gradient technique was used, and generally gave convergence to the optimum structure within 60–100 steps.

All $C_{36}H_6$ and all but 1% (17) of $C_{36}F_6$ isomers converged to local minima without change of bonding topology. The 17 cases of $C_{36}F_6$ which showed dissociation (C–F overlap population <0.3) are all intrinsically radicaloid, involve isolated sp^2 carbons, and are excluded from the comparisons made below.

5 Results

$C_{36}H_6$

Energies of the optimised structures for the full set of $C_{36}H_6$ isomers span a range of 650 kJ mol^{-1}, and as Fig. 2 shows, are distributed roughly symmetrically over this interval. The subset of symmetrical isomers covers almost exactly the same range (Fig. 2, inset), has a similar distribution and contains the globally optimal D_{3h} $C_{36}H_6$ molecule discussed in our earlier paper.[15] Although the C_1 set does not contain the best candidate, many of the low-energy isomers, including three of the best six, are without symmetry (Table 2, Fig. 3). The best isomer is characterised by a D_{3h} pattern of 1,4-addition in three disjoint equatorial hexagons of C_{36}. It has been argued[15] that the C_{36} fullerene can use these six bonding sites to behave as a 'superatom' forming strong dimers, oligomers and solids. Many of the low-energy isomers, including all of the best six, include at least two equatorial 1,4 pairs.

Comparison of the symmetrical and full sets of calculations suggests two conclusions. One is that symmetry restrictions can be risky in a search for low-energy isomers; in the present case the symmetric search captures the global minimum but misses 47 C_1 structures out of a total of 82 within the first 100 kJ mol^{-1}. The second is that, when low-energy structures have

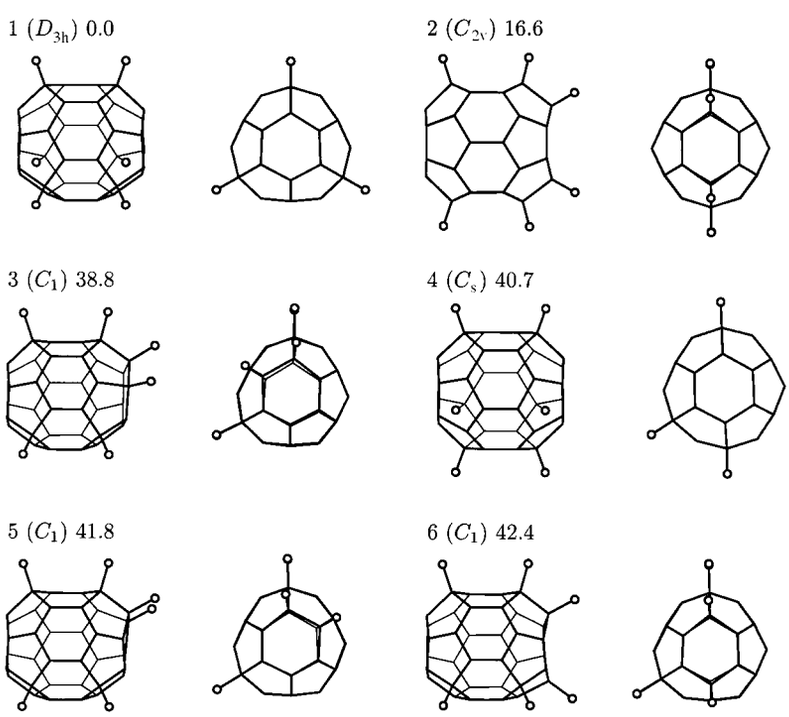

Fig. 3 Six energetically favoured isomers of $C_{36}H_6$. Each isomer is shown from two orthogonal views and labelled by molecular point group and energy relative to the best (D_{3h}) isomer. The same six topologies are used for the comparative study of $C_{36}F_6$ isomers, as reported in Table 2.

Table 2 Relative energies of $C_{36}X_6$ isomers (kJ mol^{-1}). The selected cages are the six $C_{36}H_6$ isomers of lowest energy according to DFTB calculations and their $C_{36}F_6$ analogues. Energies obtained from single-point LDA and GGA calculations are shown for comparison. All energies are given relative to the optimal D_{3h} isomer in both series. The optimised structures of the $C_{36}H_6$ isomers are illustrated in Fig. 3

		$C_{36}H_6$			$C_{36}F_6$		
	G	E_{DFTB}	E_{ELDA}	E_{GGA}	E_{DFTB}	E_{LDA}	E_{GGA}
1	D_{3h}	0.0	0.0	0.0	0.0	0.0	0.0
2	C_{2v}	16.6	20.1	32.9	18.8	8.9	12.1
3	C_1	38.8	42.8	48.4	42.2	12.9	19.2
4	C_s	40.7	43.6	44.3	49.0	48.1	48.5
5	C_1	41.8	48.9	56.9	51.9	46.1	49.8
6	C_1	42.4	44.9	51.7	43.2	32.5	34.7

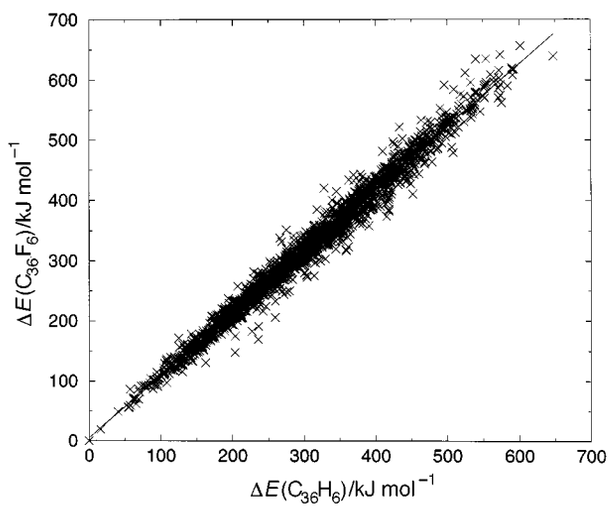

Fig. 4 Energies of hydrogenated and fluorinated fullerenes $C_{36}X_6$. All isomers with non-trivial symmetry are compared on the scatterplot taking DFTB energies relative to the appropriate D_{3h} isomer, with the regression line $[\Delta E(C_{36}F_6)/\text{kJ mol}^{-1}] = a[\Delta E(C_{36}H_6)/\text{kJ mol}^{-1}] + b$ ($a = 1.04$, $b = 4.69$ and correlation coefficient $r^2 = 0.9902$).

been identified, they may be rationalised by rather simple chemical rules that cut across symmetry classifications. In this case the rule is a preference for 1,4-addition in hexagons, which is also found elsewhere in fullerene chemistry.[30]

$C_{36}F_6$

Calculations on the 1885 fluorofullerene isomers give an energy range of 657 kJ mol^{-1}, almost exactly equal to that of the hydrofullerenes. Significantly, the same favoured D_{3h} addition pattern is predicted for both $C_{36}F_6$ and $C_{36}H_6$. The H/F parallel is much more general than this, as is shown by Fig. 4, where the relative energies of $C_{36}H_6$ and $C_{36}F_6$ cages are plotted. When the energies are taken relative to that of the best isomer in the series, a striking correlation is observed, with the slope of almost exactly unity implying a constant difference between isostructural $C_{36}H_6$ and $C_{36}F_6$ isomers. In other words, the energy cost of rearranging six C–H or six C–F bonds from their optimal D_{3h} disposition is the same, according to the DFTB model.

This parallel can be extended to the HOMO–LUMO gaps (Fig. 5), where the correlation is poorer ($r^2 = 0.889$) but is still marked when a large gap is present. Although gap and stability are not quantitatively correlated in these molecules, the correlation is best for a large gap, and it is perhaps significant that the favoured D_{3h} isomer has by far the largest gap (2.3 eV in both cases).

Comparison with full DFT calculations

The focus of the current application is on isomer energy differences, and an excellent correlation has been observed between DFTB energies of $C_{36}H_6$ and $C_{36}F_6$. This is in line with chemical expectations. However, the density in a tight-binding method is not calculated in a self-consistent way and so DFTB could, in principle, fail to account correctly for charge separation in polar bonds between elements of widely different electronegativity. In order to check whether incipent ionic character in the C–F bond has produced systematic errors in the DFTB model, fully self-consistent DFT calculations were performed for selected isomers employing both LDA and GGA methods. Single-point calculations were performed on the six $C_{36}H_6$ isomers of lowest energy according to the DFTB model, and on their isostructural $C_{36}F_6$ analogues. In each case, the energy was calculated at the higher level of theory but using the DFTB-optimised structure.

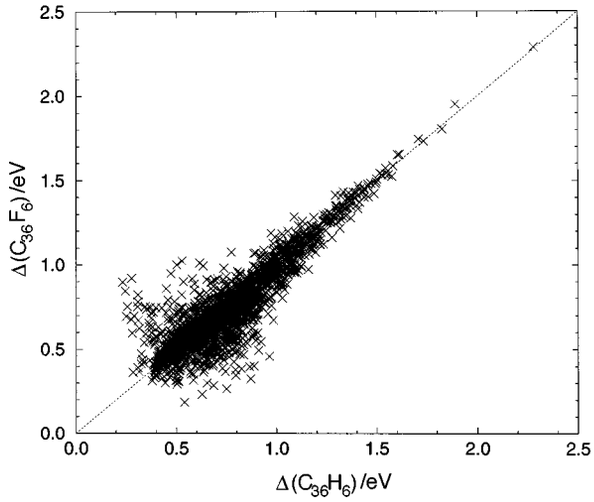

Fig. 5 HOMO–LUMO gaps of hydrogenated and fluorinated fullerenes $C_{36}X_6$. All isomers with non-trivial symmetry are represented on the scatterplot where Δ is the DFTB-computed gap in eV and the dotted line of unit slope is drawn as a guide to the eye.

Calculation of fixed-point energies at a higher level of theory using geometries optimised at a lower level is, of course, a common practice. Here it can be justified by our own tests (Section 2) and other results for carbon clusters[13,15] which show that DFTB and LDA geometries are in general close to each other and to experiment, where available (Table 1, see also ref. 31). Single-point calculations with GGA methods at LDA or similar geometries give the best mixture of energy and structure.[31]

As Table 2 shows, the overall order of isomers is similar in all three methods with the exception of isomer 3 of $C_{36}F_6$. Relative energies differ by at most ≈30 kJ mol^{-1} but more usually by much less. The systematically higher energies of the less stable isomers of $C_{36}F_6$ in the DFTB model suggest an overestimation of the stability of the best (D_{3h}) cage by ≈10 kJ mol^{-1}.

6 Conclusions

This paper reports the results of some 84 000 geometry optimisations. An extensive survey of all possible $C_{36}H_6$ and all symmetrical $C_{36}F_6$ isomers has confirmed that the thermodynamically favoured structure in each case has D_{3h} symmetry, accounted for by a simple chemical rule of 1,4-addition which also rationalises the other low-lying isomers of lower symmetry. The proposed tendency to parallel energy for isostructural hydrogenated and fluorinated fullerenes is confirmed by this large set, suggesting that it may be general amongst fullerene derivatives. The new parameterisation of DFTB opens up the possibility of further exploration of the factors influencing fluorofullerene stability.

7 Acknowledgements

The authors wish to thank Vitus Servedio of the Max-Planck-Gruppe für korrelierte Systems der TU Dresden for the calculation of the LDA-LSDA energy differences. Financial support from EPSRC, the DAAD/British Council project ARC 868 and the European Union TMR Network 'USEFULL' (FMRX-CT97-0126) is gratefully acknowledged.

References

1 R. E. Haufler, J. Conceicao, L. P. F. Chibante, Y. Chai, N. E. Byrne, S. Flanagan, M. M. Haley, S. C. O'Brien, C. Pan, Z. Xiao, W. E. Billups, M. A. Ciufolini, R. H. Hauge, J. L. Margrave, L. J. Wilson, R. F. Curl and R. E. Smalley, *J. Phys. Chem.*, 1990, **94**, 8634.
2 F. N. Tebbe, R. L. Harlow, D. B. Chase, D. L. Thorn, G. C. Campbell, J. C. Calabrese, N. Herron, R. J. Young and E. Wasserman, *Science*, 1992, **256**, 822.
3 P. R. Birkett, P. B. Hitchcock, H. W. Kroto, R. Taylor and D. R. M. Walton, *Nature*, 1992, **357**, 479.
4 P. R. Birkett, A. G. Avent, A. D. Darwish, H. W. Kroto, R. Taylor and D. R. M. Walton, *J. Chem. Soc.*, *Chem. Commun.*, 1995, 683.
5 O. V. Boltalina, V. Y. Markov, R. Taylor and M. P. Waugh, *Chem. Commun.*, 1996, 2549.
6 P. W. Fowler, J. P. B. Sandall and R. Taylor, *J. Chem. Soc.*, *Perkin Trans. 2*, 1997, 419.
7 P. W. Fowler, T. Heine, D. E. Manolopoulos, D. Mitchell, G. Orlandi, R. Schmidt, G. Seifert and F. Zerbetto, *J. Phys. Chem.*, 1996, **100**, 6984.
8 P. W. Fowler, T. Heine, D. Mitchell, G. Orlandi, R. Schmidt, G. Seifert and F. Zerbetto, *J. Chem. Soc.*, *Faraday Trans.*, 1996, **92**, 2203.
9 A. Ayuela, P. W. Fowler, D. Mitchell, R. Schmidt, G. Seifert and F. Zerbetto, *J. Phys. Chem.*, 1996, **100**, 15634.
10 M. C. Domene, P. W. Fowler, D. Mitchell, G. Seifert and F. Zerbetto, *J. Phys. Chem. A*, 1997, **101**, 8339.
11 P. W. Fowler, T. Heine, D. Mitchell, R. Schmidt and G. Seifert, *J. Chem. Soc.*, *Faraday Trans.*, 1996, **92**, 2197.
12 P. W. Fowler, K. M. Rogers, G. Seifert, M. Terrones and H. Terrones, *Chem. Phys. Lett.*, 1999, **299**, 359.
13 D. Porezag, T. Frauenheim, T. Köhler, G. Seifert and R. Kaschner, *Phys. Rev. B*, 1995, **51**, 12947.
14 C. Piskoti, J. Yarger and A. Zettl, *Nature*, 1998, **393**, 771.
15 P. W. Fowler, T. Heine, K. M. Rogers, J. P. B. Sandall, G. Seifert and F. Zerbetto, *Chem. Phys. Lett.*, 1999, **300**, 369.
16 P. Hohenberg and W. Kohn, *Phys. Rev. B*, 1964, **136**, 848.
17 W. Kohn and L. J. Sham, *Phys. Rev. A*, 1965, **140**, 1133.
18 H. Eschrig and I. Bergert, *Phys. Status Solidi B*, 1978, **90**, 621.
19 G. Seifert, D. Porezag and T. Frauenheim, *Int. J. Quantum Chem.*, 1996, **58**, 185.
20 G. Seifert and R. O. Jones, *Z. Phys. D*, 1991, **20**, 77.
21 A. M. Köster, M. Krack, M. Lebœuf and B. Zimmermann, *AllChem*, 1998, Universität Hannover.
22 S. H. Vosko, L. Wilk and M. Nusair, *Can. J. Phys.*, 1980, **58**, 1200.
23 N. Godbout, D. R. Salahub, J. Andzelm and E. Wimmer, *Can. J. Chem.*, 1992, **70**, 560.
24 A. D. Becke, *Phys. Rev. A*, 1988, **38**, 3098.
25 C. Lee, W. Yang and R. G. Parr, *Phys. Rev. B*, 1988, **37**, 785.
26 V. Servedio, personal communication.
27 J. P. Perdew and A. Zunger, *Phys. Rev. B*, 1981, **23**, 5048.
28 D. R. Lide, ed., *CRC Handbook of Chemistry and Physics*, Chemical Rubber Publishing Co., Boca Raton, Florida, 1992. Experimental data for the bond lengths and angles are for organic molecules in the gas phase, measured by electron diffraction. The F–F bond length was determined by Raman spectroscopy.
29 P. W. Fowler and D. E. Manolopoulos, *An Atlas of Fullerenes*, Oxford University Press, New York, 1995.
30 S. J. Austin, P. W. Fowler, J. P. B. Sandall, P. R. Birkett, A. G. Avent, A. D. Darwish, H. W. Kroto, R. Taylor and D. R. M. Walton, *J. Chem. Soc.*, *Perkin Trans. 2*, 1995, 1027.
31 P. Calaminici, A. M. Köster, N. Russo and D. R. Salahub, *J. Chem. Phys.*, 1996, **105**, 9546.

Paper 9/00471H